Journal of Alloys and Compounds 773 (2019) 277–287

Contents lists available at ScienceDirect

Journal of Alloys and Compounds

journal homepage: http://www.elsevier.com/locate/jalcom

Microstructural mechanisms during multidirectional isothermal forging of as-cast Ti-6Al-4V alloy with an initial lamellar microstructure

Z.X. Zhang [a, b], S.J. Qu [a, *], A.H. Feng [a], X. Hu [c], J. Shen [a]

[a] School of Materials Science and Engineering, Tongji University, Shanghai 201804, PR China
[b] College of Mechanical Engineering, Taiyuan University of Technology, Taiyuan 030024, PR China
[c] Aerospace Industry LLC, Shifang 618400, PR China

ARTICLE INFO

Article history:
Received 18 April 2018
Received in revised form
14 September 2018
Accepted 17 September 2018
Available online 18 September 2018

Keywords:
Ti-6Al-4V alloy
Isothermal forging
Microstructure

ABSTRACT

Microstructural evolution and tensile properties of Ti-6Al-4V alloy with an initial lamellar microstructure during the multidirectional isothermal forging (MDIF) were investigated. After three steps isothermal forging, a homogeneous equiaxed grained microstructure with an average grain size of 1.9 μm was achieved. The grain refinement mechanism included both continuous dynamic recrystallization (CDRX) and discontinuous dynamic recrystallization (DDRX). The necklaces of new DDRX grains with high angle grain boundaries (HAGBs) were formed along the initial β grain boundaries. Grain subdivision was through CDRX. The fraction of recrystallization and the homogeneity of microstructure were improved with the isothermal forging steps increasing, the fractions of recrystallization increased from 43% to 63% and the fractions of HAGBs increased from 48% to 71%, respectively. The tensile properties of as-cast Ti-6Al-4V alloy were significantly improved at both room temperature and 400 °C, respectively. The yield strength, ultimate tensile strength and elongation increased 21%, 23%, and 210% at room temperature, respectively. And at 400 °C, the yield strength, ultimate tensile strength and elongation increased 46%, 48%, and 21%, respectively. The fracture mechanism changed from brittle fracture to ductile fracture after the MDIF process.

1. Introduction

Ti-6Al-4V alloy is one of the most important titanium alloys and has been used extensively in aerospace, biomedical and energy related industries for structural applications due to its specific high strength-to-weight ratio, good ductility, good biocompatibility and relatively low cost [1–6]. Microstructure has an important influence on the properties of the alloy, control and optimization of the microstructure is significant in achieving desired mechanical properties. Thermomechanical processing is the most useful method to modify the microstructure [7–9]. The Ti-6Al-4V alloy is commonly produced by the way of ingot metallurgy [10]. Hot working processes of as-cast ingots to modify the β transformed microstructure into an equiaxed α+β structure forms the first and most important step in the manufacturing of Ti-6Al-4V components [11–14]. Hot working processes conducted in the α+β field (including extrusion [15], forging [16,17] and hot rolling [8]) are the main approaches to breakdown the lamellar structure.

MDIF is applied for the ultrafine-grained (UFG) structures in large billets [18]. In our previous work, with the change of the loading directions during the MDIF, a homogeneous UFG structure with an average grain size of ~0.5 μm has been achieved in Ti-6Al-4V alloy [4]. The process of MDIF is generally associated with dynamic recrystallization (DRX) [19]. Therefore, the MDIF process could be effective to transform the lamellar structure into the equiaxed structure in Ti-6Al-4V alloy.

Various investigations have been made to provide insight into the possible mechanisms of globularization of lamellar structure [16,20–25]. Weiss et al. [16] identified two different boundary splitting mechanisms contributing to the fragmentation of lamellae during forging. Both involve the formation of boundaries across individual alpha lamellae. The main driving force was hypothesized to the intense shear bands or the formation of a recovered substructure. In summary, the globular α grains result from the process

* Corresponding author.
E-mail address: qushoujiang@tongji.edu.cn (S.J. Qu).

https://doi.org/10.1016/j.jallcom.2018.09.220
0925-8388/

Table 1
Chemical composition of as-cast Ti-6Al-4V alloy (wt. %).

	Ti	Al	V	Si	C	O	N	H	Fe
wt.%	Bal.	6.08	4.03	0.013	0.018	0.11	0.0047	0.0008	0.14

of globularization of α lamellae, which is considered as a type of DRX. However, these investigations are mainly through uniaxial deformation, studies on the DRX during the multidirectional deformation are limited.

Besides the microstructure, crystallographic textures also have a large effect on the mechanical properties of the Ti-6Al-4V alloy [10,26,27]. Recently, large regions of grains with similarly orientations have been usually found in titanium alloys, known as macrozones [8]. These microtextured regions were considered as sites of multiple initiating cracks [28]. Current research suggests that microtexture is more critical to in-service lifetimes of Ti-6Al-4V components than microstructure [29]. Furthermore, the texture development is influenced by the mode of deformation [16]. The information about the microtexture development of Ti-6Al-4V alloy during MDIF is still limited.

The objective of this study is to achieve a homogeneous equiaxed grained microstructure in Ti-6Al-4V alloy with an initial lamellar microstructure through MDIF, and to examine the microstructural mechanisms and microtexture development during MDIF. The effect of MDIF process on the tensile properties of as-cast Ti-6Al-4V was investigated in detail. The mechanisms of dynamic recrystallization and the evolution of deformation microtextures were investigated.

2. Materials and methods

2.1. Materials

The material used in this study was extra-low interstitial (ELI) grade as-cast Ti-6Al-4V alloy billet. The chemical composition of the alloy was shown in Table 1. The β transus temperature of this alloy was reported to be ~975 °C [30]. As-received bar with a diameter of 355 mm and a length of 550 mm was produced by ingot metallurgy.

2.2. Experimental procedures

MDIF was used to achieve grain refinement in as-cast Ti-6Al-4V alloy. As shown in Fig. 1a, the MDIF process consisted of three steps forging. Prior to the second step forging, the pancake produced in the first step isothermal forging was canted through cutting the curved faces off the billet, and rotating the pancake by 90°. The process of the third step isothermal forging was the same. The MDIF was developed at temperature range of 995 °C–850 °C. In order to obtain the finest grain, the forging temperature should be lowered as much as possible. Due to the improvement in the hot workability of the Ti-6Al-4V alloy resulted from microstructural refinement, the forging temperature in the next step was lowered by 50–100 °C. After the first step isothermal forging, a recrystallization annealing was conducted at 900 °C for 30 min to promote the recrystallization of the alloy. Details of MDIF process were summarized in Table 2. Initially, cylindrical samples (Φ 60 × 100 mm^2) were prepared by electrospark wire-electrode cutting.

As shown in Fig. 1b, the samples for microstructural examination after the first step and the second step isothermal forging were taken from the middle area of the leftover materials. The samples for microstructural examination were taken from the middle area in the longitudinal section of the isothermal forged billets. The middle area is representative and is convenient for comparison. The locations of microstructure specimens after the third step isothermal forging were given in Fig. 1c.

The microstructure was examined by using optical microscopy (OM, Carl Zeiss Axio Observer. 5m), scanning electron microscopy (SEM, FEI Quanta 250 FEG), and thermal field emission scanning electron microscopy (EBSD, Apollo 300). The specimens were electrochemically polished for OM, SEM, EBSD characterization. A solution consisting of 60% methanol, 34% *n*-butanol, and 6% perchloric was used for the electrochemically polishing. The process of electrochemically polishing was conducted with an applied current of 90 mA at −30 °C. In this work, the β phase is too difficult to well-indexed, thus, the EBSD data including grain diameter distribution charts, misorientation angle distribution charts and pole figures were analyzed only for α phase. The recrystallized grains which were represented by the blue area were separated by the high angle grain boundaries (HAGBs). High angle grain boundaries (HAGBs) were defined as grain boundaries with

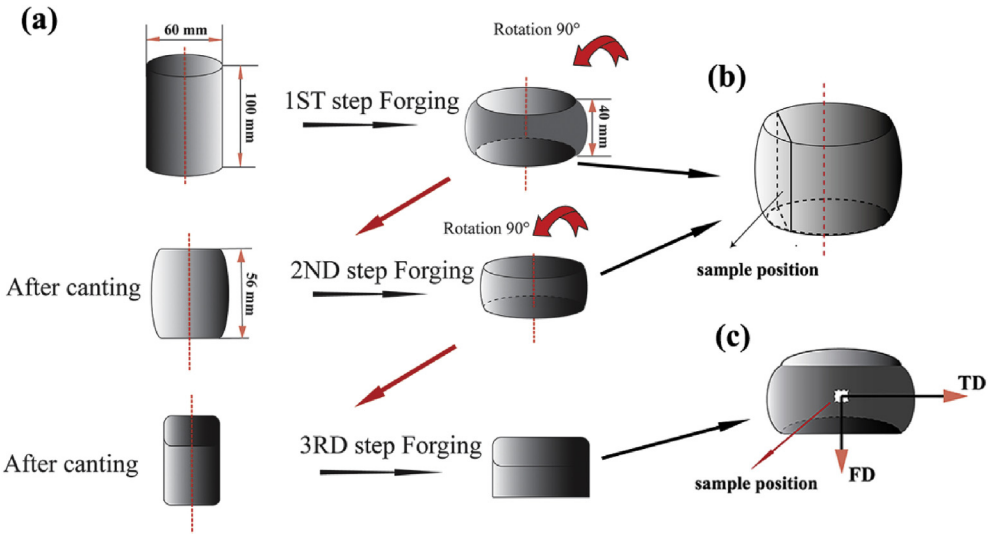

Fig. 1. (a) Schematic diagram of multidirectional isothermal forging, and viewing position of specimens: (b) after the first and second step isothermal forging, (c) after the third step isothermal forging.

Table 2
MDIF parameters of Ti–6Al–4V alloy.

Isothermal forging step	MDIF parameters			
	Temperature (°C)	Strain rate (s^{-1})	ISF reduction (%)	Cooling conditions
1st step isothermal forging	995	1×10^{-2}	60	AC After RA
2nd step isothermal forging	950	1×10^{-3}	50	AC
3rd step isothermal forging	850	1×10^{-3}	70	AC

Note: Isothermal forging: ISF; AC: air cooling; RA: recrystallization annealing: 900 °C/0.5 h.

misorientation above 15°. The substructures which were represented by the green area were separated by the low angle grain boundaries (LAGBs). Low angle grain boundaries (LAGBs) were defined as the grain boundaries with misorientation between 3° and 15°. The deformed structures which were represented by the red area were separated by the grain boundaries with misorientation below 3°.

Tensile tests were conducted on the Zwick Z100 servohydraulic testing system at an initial strain rate of 10^{-3} s^{-1}. Plate specimens with a width of 4 mm, a thickness of 2 mm, and a gauge length of 14 mm were employed.

3. Results and discussion

3.1. As received materials

Fig. 2 shows the initial microstructure of the as-cast Ti-6Al-4V alloy. It was a typical Widmanstätten structure consisting of large prior β grains of the order of mm. The primary α layer at the initial β grain boundaries was 5 μm thick. The lamellar α colonies were formed inside the prior β grains and the thickness of α laths was about 3 μm thick. The thickness of the retained thin β layer between the primary α was about 1 μm thick. The EBSD measurement results of as-cast Ti-6Al-4V alloy were shown in Fig. 2d and e. As shown in Fig. 2d, similarly orientated α colonies developed into macrozones, represented by regions with different colours. It is considered as a result of ingot processing [8].

3.2. Mechanism of refinement of the microstructure

As shown in Fig. 3, after the first step isothermal forging process, the initial β grains were not vanished completely, the grain boundaries were retained. Furthermore, during the deformation, the grain boundaries were partial broken up and kinked (Fig. 3a).

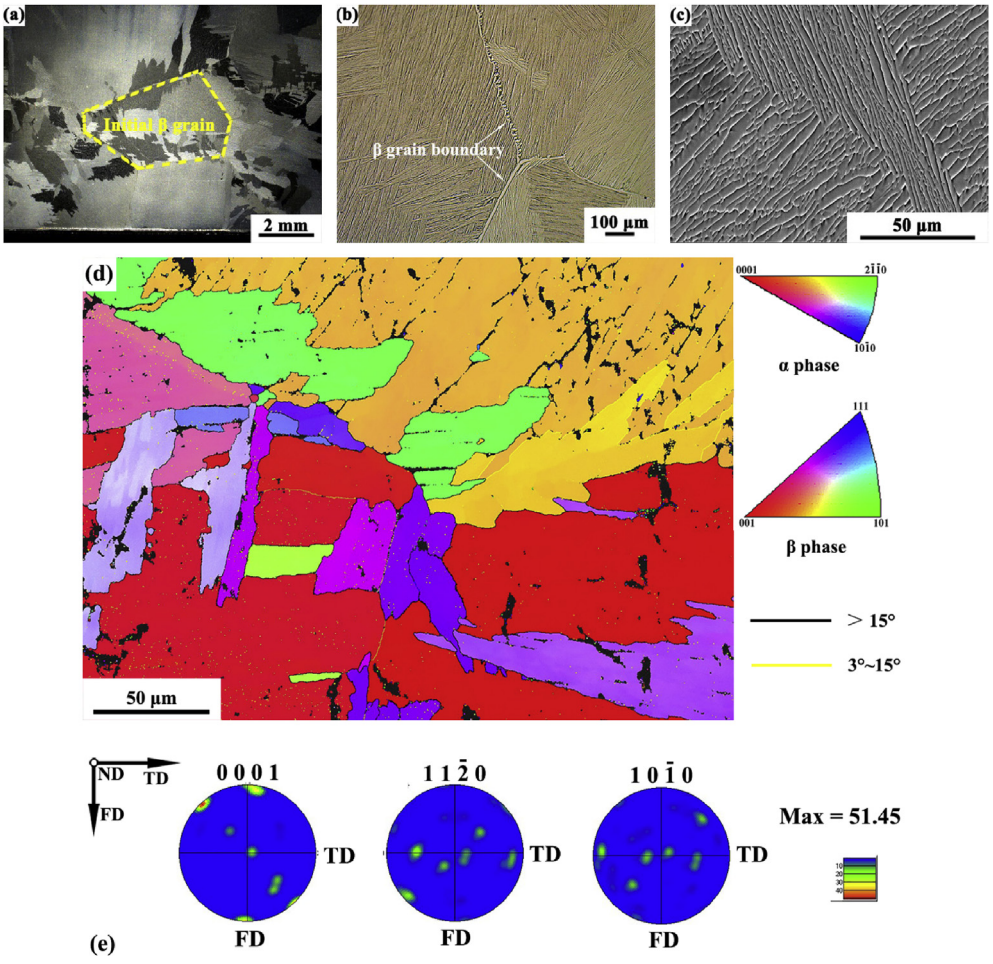

Fig. 2. As-received Ti-6Al-4V alloy: (a) macro picture, (b) OM image, (c) SEM image, (d) the orientation map, and (e) pole figure of α phase.

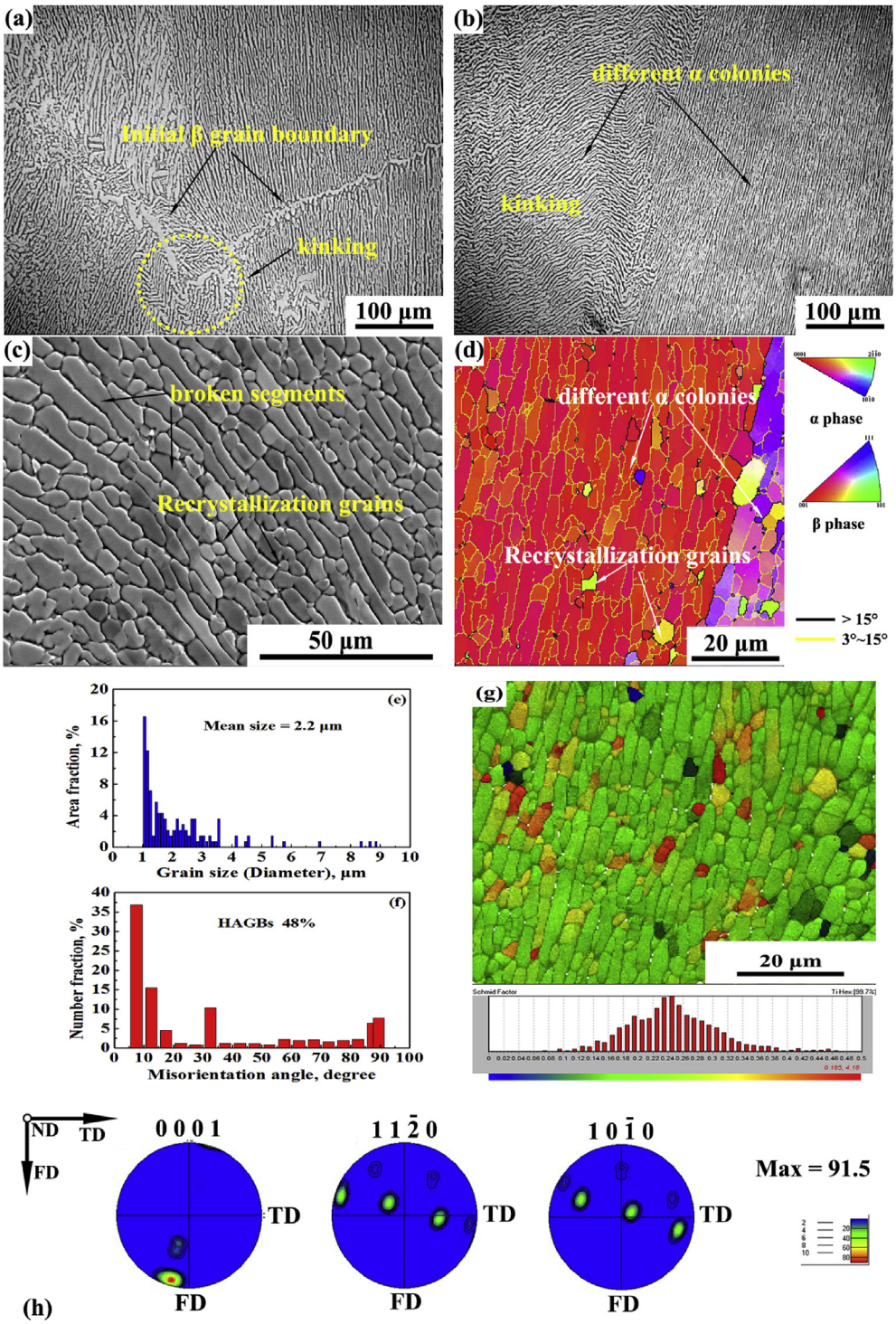

Fig. 3. Microstructure of Ti-6Al-4V alloy after the first step isothermal forging, (a), (b) OM images, (c) SEM image, (d) the orientation map, (e) grain size diameter distribution chart of α phase, (f) misorientation angle distribution chart of α phase, (g) Schmid factor distribution map, and (h) pole figure of α phase.

The first step isothermal forging was aimed to break down the coarse as-cast microstructure. The breakdown of the transformed β microstructure during hot deformation plays a key role to develop a desired equiaxed microstructure. Because of its great importance, a lot of work has been done to give sight in the conversion of transformed β microstructure to the desired equiaxed microstructure [15,16,21,27,31]. It needs great process control to avoid the microstructural defects happening. Chen et al. [31] investigated the deformation characteristics of Ti-6Al-4V alloy with transformed β microstructure under isothermal forging conditions. In their work, after forging both the Widmanstätten and grain boundary α appeared kinked, suggesting the α phase recrystallization. Weiss et al. [16] investigated the modification of lamellar α phase of Ti-6Al-4V alloy through hot forging, the investigation results indicated that the effect of processing parameters and initial microstructure on the process of globularization of lamellar structure, the

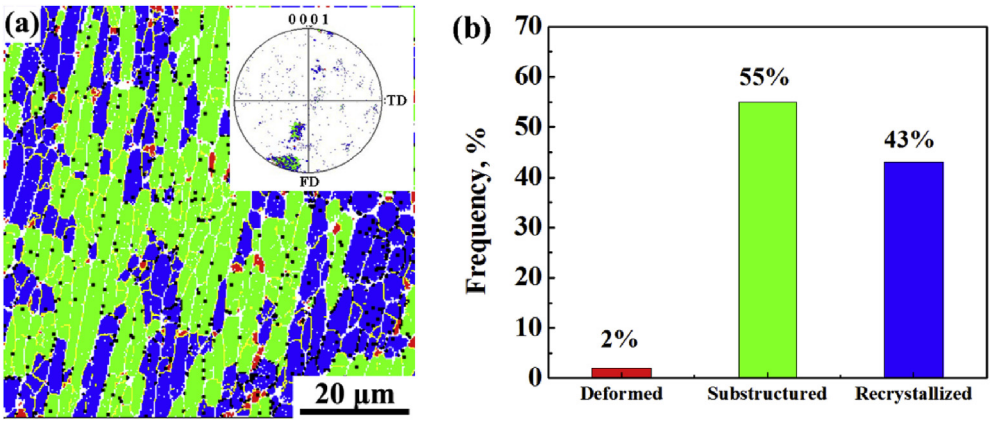

Fig. 4. The extent of recrystallization after the first step isothermal forging, (a) recrystallized image, (b) recrystallized fraction chart.

aspect ratio of the α phase decreased with the deformation strain increasing and thin α lamellae was more easily to globularized. Semiatin [27] also reported that in order to get a microstructure consisting of fine equiaxed primary α phase and transformed β, the billets should be hot deformed below the β transus. Brun et al. [32] noted that the development of a regulated structure in α+β two phase titanium alloy was significant for the production of titanium alloy semiproducts and needed a controlled hot deformation in the β phase field or in α+β phase field followed by a recrystallization annealing. Thus, during the MDIF process, the first step isothermal forging was conducted in the β phase field. Besides, since the temperature of the forging die was below the β transus temperature, considering the effect of die-chilling during forging, the primary ingot breakdown was considered to finish at a temperature below the β transus temperature.

As shown in Fig. 2, one initial β grain was consisted of several colonies comprising of α lamellae with different orientations. The changes of the microstructure morphology of the α+β two phase titanium alloy depends on the initial orientation of the α lamellae [33]. During the one step isothermal forging, the loading direction was vertical, the α lamellae with favorably orientation (*c*-axis tilts of 15–75°) or less favorably orientation (*c*-axis tilts of 20 or 75°) became kinked [33]. However, some areas with very hard orientation (with the *c*-axis tilted less than 15°) had little change in the microstructure morphology and the lamellar structure were retained (Fig. 3b). As shown in Fig. 3c, due to the isothermal forging process, the lamellar structure was broken down and converted to small segments. Several segments were globularized to form recrystallized grains in the annealing process. In addition, as shown in Fig. 3d, though the lamellar structure was broken down, α colonies were remained because of the same orientation, the retained α lamellae have the same orientation to form two macrozones (Fig. 3d), the lamellar segments of α phase were mainly surrounded by the low angle grain boundaries (LABGs) (which referred to yellow lines), which means that α segments inside the colonies are still subgrains and not recrystallized. The recrystallized grains were distributed in the matrix and surrounded by the HAGBs (which were represented by the black lines). And as shown in Fig. 3e, the average grain size of the recrystallized α grains was 2.2 μm. In addition, the fraction of the HAGBs (Fig. 3f) was relatively low (~48%), which was in good agreement with the observations in Fig. 3d. The Schmid factor distribution map was shown in Fig. 3g. The Schmid factor varied from 0.08, represented as blue, to 0.46, represented as red, with intermediate values represented as green. Grains in Fig. 3g were mostly represented by green, it indicates that the c-axis is perpendicular to the forging axis, namely, grains have "hard" orientation. The regions with lower Schmid factors correlate with regions that resisted breakdown. As shown in Fig. 3h, the microtextures of the two α colonies were indicated in the pole figures, the stronger component corresponds to the red area in Fig. 3d while the weaker component corresponds to the purple area. The red colour in Fig. 3d indicates that the *c*-axis is parallel to the forging direction, this macrozone runs parallel to the forging direction and extends for many micrometers along the sample. The texture intensity was about 91.5, it indicates that the α texture appears intensive.

The recrystallization behavior of Ti-6Al-4V alloy during MDIF process was investigated via EBSD examination. After the first step isothermal forging, the extent of recrystallization was shown in Fig. 4, the recrystallized volume fraction was ~43% (Fig. 4b).

For the second step isothermal forging, the loading direction was tilted by 90° and the temperature was decreased by 45 °C. After the second step isothermal forging, the initial β grains were nearly disappeared, and the grain boundaries were broken up to small segments and only a few were retained (Fig. 5a). During the MDIF, the deformation is conducted with sequential changes of loading direction. Thus, various slip systems operate at each forging step. As a consequence, α colonies with different orientations can undergo the process of globularization. The MDIF process can accelerate the globularization of α lamellae. After the second step isothermal forging, with the change of loading direction by 90°, α colonies with different orientations became kinked and globularized, as shown in Fig. 5b. The retained α lamellae were further refined (Fig. 5c and d). As shown in Fig. 5d, subgrains surrounded by the LAGBs were formed in the globularized grains, which suggested that the subdivision of the grains was through the transformation of the dislocation sub-boundaries into globularized grains HAGBs. This process was termed CDRX. Besides, the necklaces of new grains formed along the grain boundaries were observed, which was a typical microstructure developed during the process of DDRX. This result clearly indicated that the DRX process included both CDRX and DDRX. The average grain size was 3.1 μm and the fraction of the HAGBs was up to 80% (Fig. 5e and f). The Schmid factor distribution map was shown in Fig. 5g. It is obvious that the Schmid values increase after the second isothermal forging. The regions with high Schmid factor were easier to breakdown with the c-axis tilted between 15 and 75°.

Furthermore, compared to the first step isothermal forging, the texture intensity was decreased (Fig. 5h), the MDIF resulted in the weakening of the microtexture, the intensity of microtexture decreased. In addition, as shown in Fig. 6, the recrystallized volume fraction was increased to 60%.

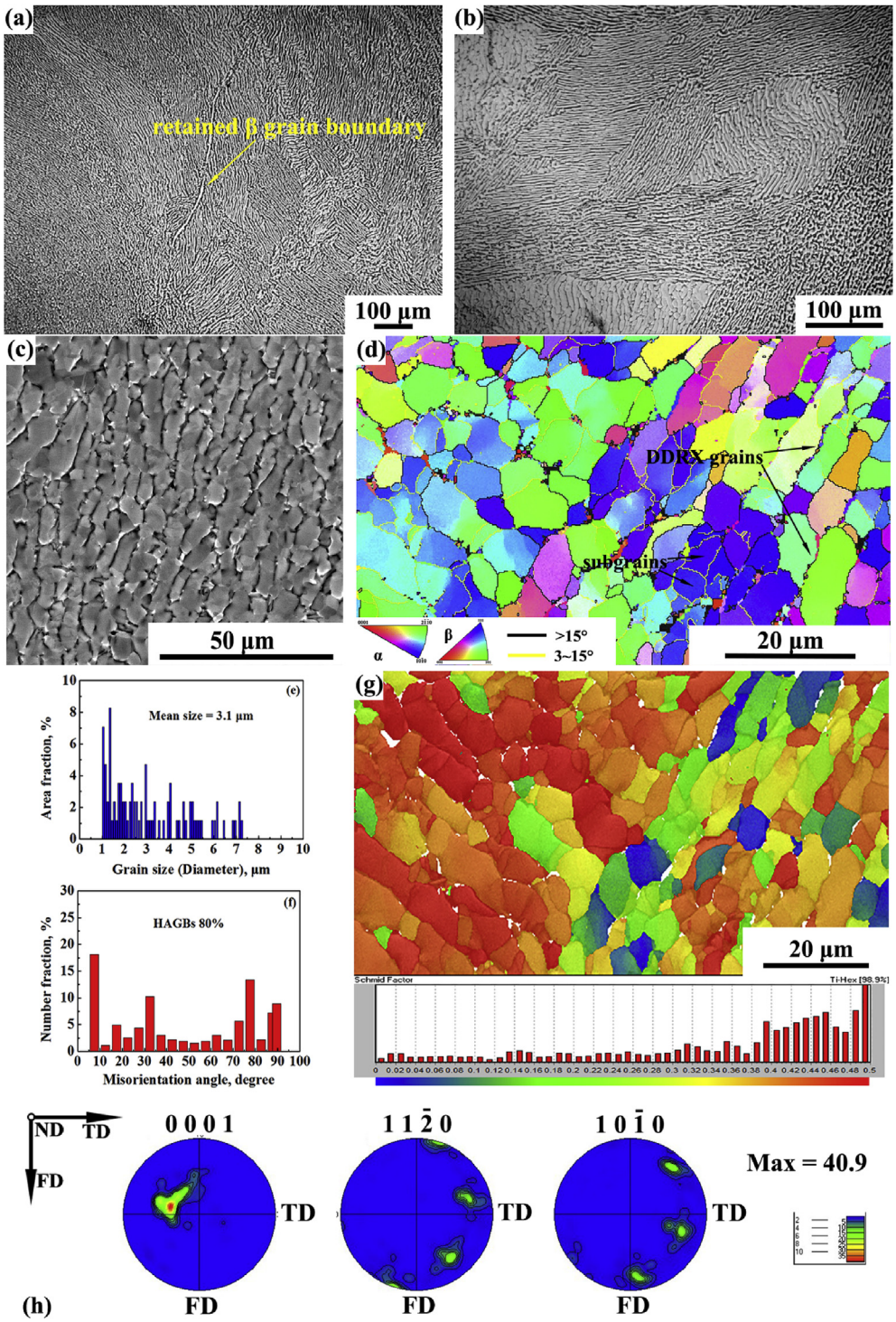

Fig. 5. Microstructure of Ti-6Al-4V alloy after the second step isothermal forging, (a), (b) OM image, (c) SEM image, (d) the orientation map, (e) grain size diameter distribution chart of α phase, (f) misorientation angle distribution chart of α phase, (g) Schmid factor distribution map, and (h) pole figure of α phase.

At the third step isothermal forging, the loading direction was tilted by 90° continuously, and the temperature was decreased to 850 °C. After three steps isothermal forging, the lamellar α structures were globularized completely. A homogenous microstructure with an average grain size of 1.9 μm was formed, and the fraction of HAGBs was 71%, furthermore, the texture intensity was decreased to 16 (Fig. 7). Similar to Fig. 5, the Schmid values increase (Fig. 7e), suggesting the higher globularization efficiency of the lamellae. The recrystallized volume fraction was increased to 63% (Fig. 8).

As indicated in Figs. 4, 6 and 8, the recrystallized fraction was 43% after the first step forging, 60% after the second step isothermal forging, and 63% after the third step isothermal forging. The results indicated that the MDIF process could accelerate the DRX of Ti-6Al-4V. Furthermore, the new recrystallized grains were similarly orientated to the substructured area, suggesting a DRX via progressive subgrain rotation [34]. This process was considered to be

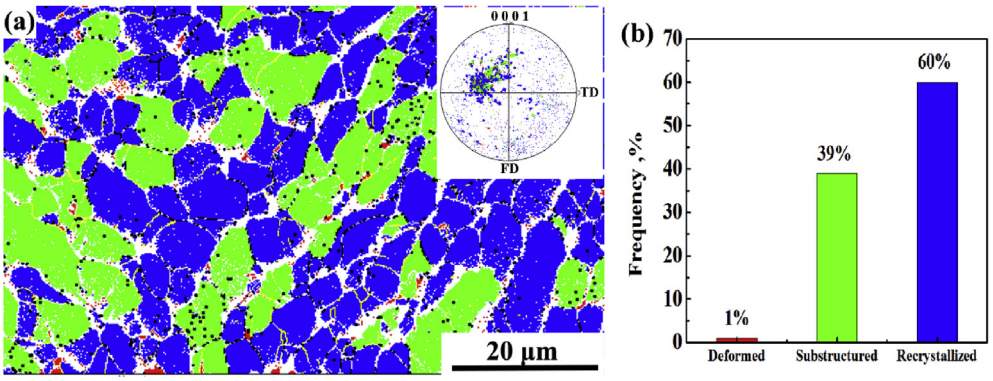

Fig. 6. The extent of recrystallization after the second step isothermal forging, (a) recrystallized image, (b) recrystallized fraction chart.

the CDRX. The results indicated that the process of globularization of lamellar structure could also be regarded as CDRX.

During hot working process, the production of new grains result from the creation of recrystallization nuclei, continued by the migration of their boundaries. This process is generally referred to be DDRX. However, under the condition of severe plastic deformation, the new grains result from the gradual transformation of the dislocation substructures produced by the deformation, which

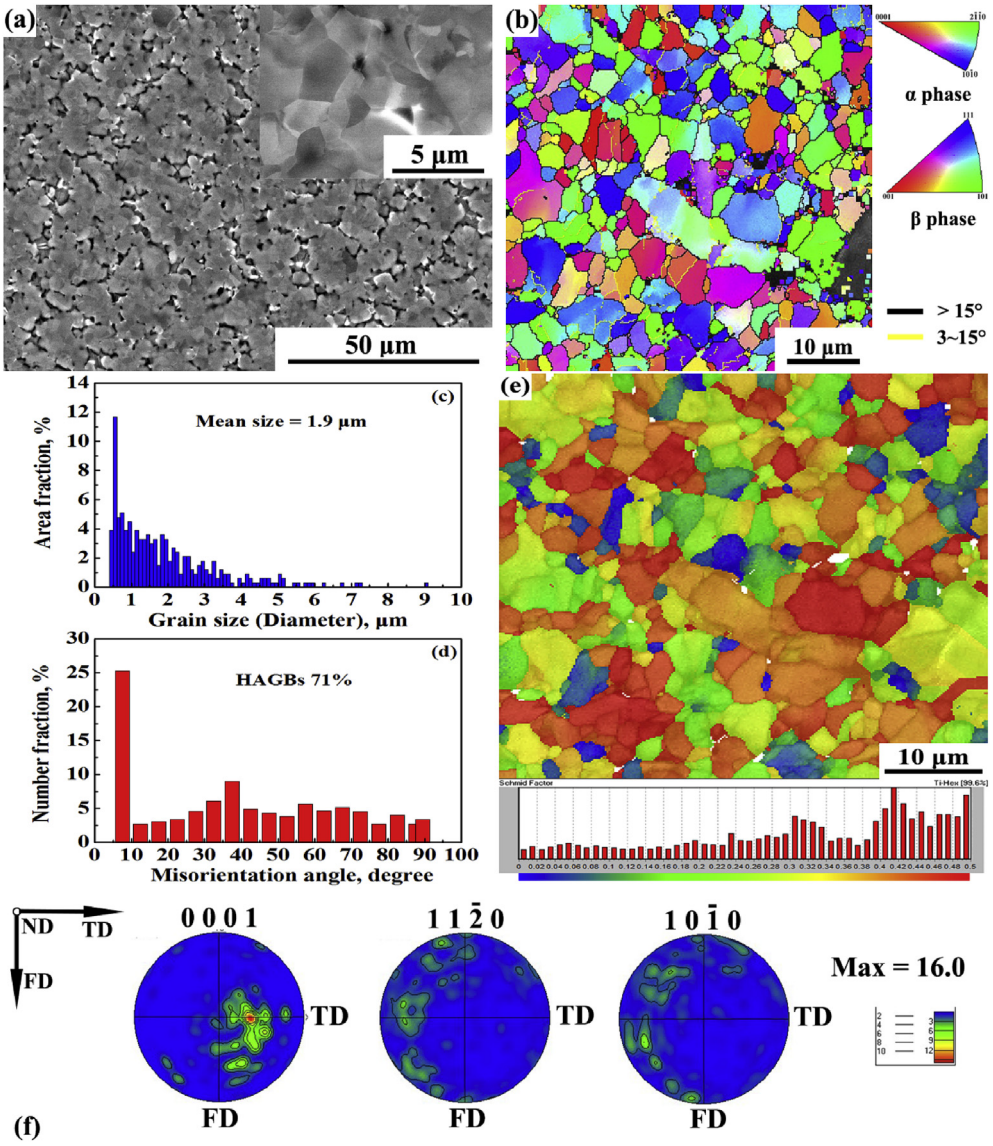

Fig. 7. Microstructure of Ti-6Al-4V alloy after the third step isothermal forging, (a) SEM image, (b) the orientation map, (c) grain size diameter distribution chart of α phase, (d) misorientation angle distribution chart of α phase, (e) Schmid factor distribution map, and (f) pole figure of α phase.

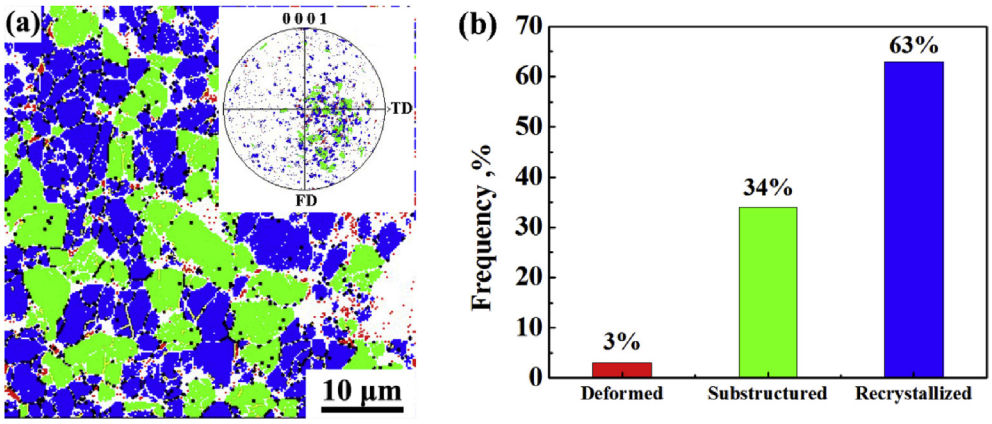

Fig. 8. The extent of recrystallization after the third step isothermal forging, (a) recrystallized image, (b) recrystallized fraction chart.

is considered to be CDRX. Matsumoto et al. [35] has investigated the microstructure conversion of Ti-6Al-4V alloy with an α'martensite starting microstructure during hot deformation. According to their results, the new DDRX grains surrounded by HAGBs were formed at the interface of martensite variants, and the CDRX occurred inside the martensite variants. Especially, during the MDIF, as reported by Zhang [4], the grain refinement mechanism of Ti-6Al-4V alloy with an α'martensite starting microstructure included both DDRX and CDRX. On one hand, grain subdivision was via CDRX, on the other hand, new DDRX grains formed along the boundaries. The CDRX process characterized by gradual transformation of dislocation cells formed at low strains into fine grains with HAGBs at high strains [4,36]. In the case of the α+β lamellar starting microstructure, it has been widely reported that the change of the microstructure during hot deformation was mainly through CDRX [25]. However, as observed in Fig. 5d, the necklaces of new grains surrounded by HAGBs formed along the boundaries. Besides, subgrains surrounded by LAGBs formed inside the grains, suggesting that grain subdivision was continued by the transformation of dislocation substructures. Above all, the grain refinement process of lamellar structure in Ti-6Al-4V included both DDRX and CDRX.

3.3. Mechanical properties at RT and 400 °C

The tensile properties at room temperature and 400 °C were summarized in Table 3, and the tensile tests engineering stress-engineering strain curves are shown in Fig. 9. As shown in Table 3, the tensile properties of as-received Ti-6Al-4V alloy at both room temperature and 400 °C were very poor. The as-cast microstructure of Ti-6Al-4V alloy produced by air-cooling from above the α+β/β transformation temperature consists of coarse (of the order of a few mm) initial β grains with Widmanstätten α+β colonies with different orientations. In addition, the segregation of β stabilizing elements (Fe, Cr, Mn, V, Cu) could result in the formation of β flecks [27]. Due to the coarse microstructure and maybe an inhomogeneity of the as-cast alloy, the mechanical properties of the as-cast Ti-6Al-4V alloy are very poor.

After three steps isothermal forging, at room temperature, the yield strength (YS) and the ultimate tensile strength (UTS) increased from 742 MPa and 747 MPa to 900 MPa and 921 MPa,

Table 3
Summary of tensile properties in Ti-6Al-4V alloy at different conditions.

	Test temperature (°C)	UTS (MPa)	YS (MPa)	El. (%)	Reduction area (%)
As-cast	RT	747	742	3.9	10
	400	417	366	10.6	38
MDIF-3rd	RT	921	900	12.1	69
	400	617	533	12.8	58

RT: room temperature.

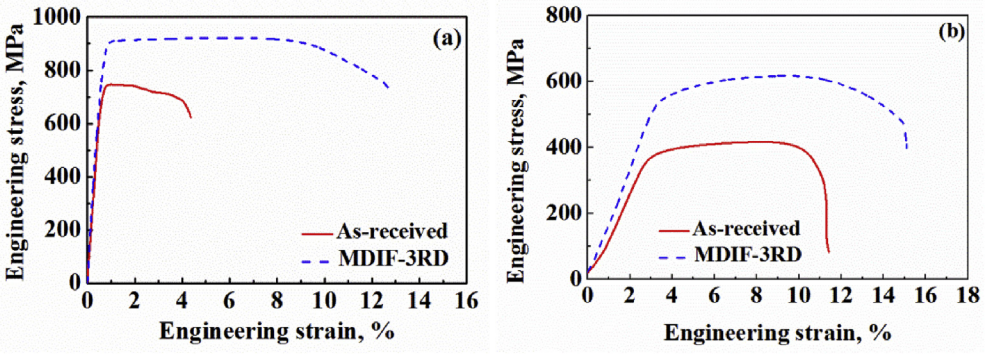

Fig. 9. Tensile engineering stress-strain curves of Ti-6Al-4V alloy at, (a) room temperature, (b) 400 °C.

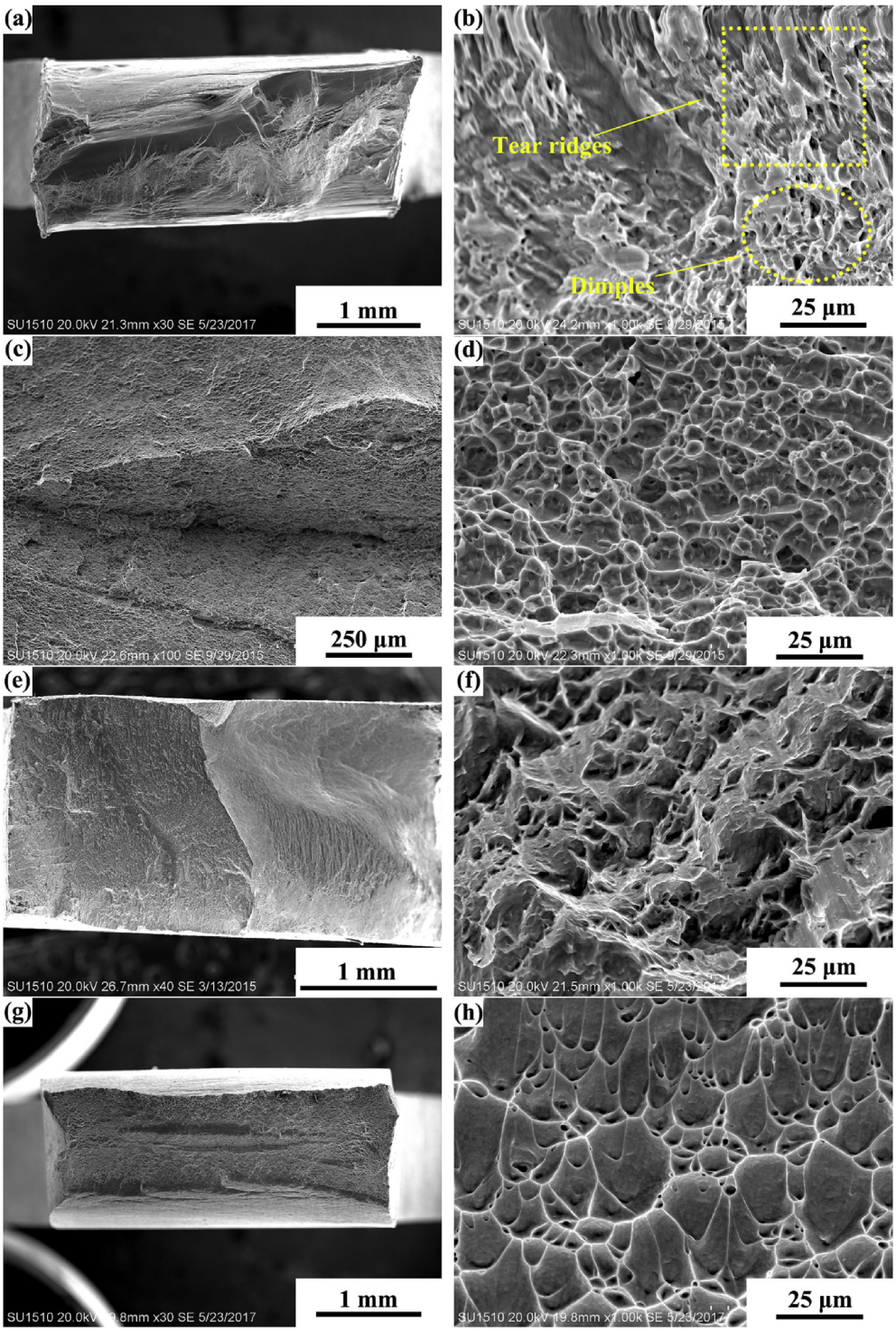

Fig. 10. SEM images showing fracture surfaces of Ti-6Al-4V alloy under different conditions, (a), (b) as-received alloy at room temperature, (c), (d) the alloy after MDIF at room temperature, (e), (f) as-received alloy at 400 °C, (g), (h) the alloy after MDIF at 400 °C.

respectively. Meanwhile, the elongation increased from 3.9% to 12.1%. The YS and UTS increased from 366 MPa and 417 MPa to 533 MPa and 617 MPa, respectively, and the elongation also increased from 10.6% to 12.8%.

It has been widely accepted that the strength properties of polycrystalline materials should depend on their grain size [37]. As a result, the strength of Ti-6Al-4V alloy increased with the grain size decreasing, thus, the mechanism of mechanical properties enhancement is considered to be grain boundary strengthening. This relation can be described by the typical Hall-Petch equation: $\sigma_y = \sigma_0 + k_y d^{-1/2}$, where σ_y is the yield stress, k_y is a constant of yielding, σ_0 is the lattice friction stress and d is the grain size. As reported by Sabirov et al. [38], grain boundaries generally act as obstacles to dislocations passing from one grain into another, resulting in the pile up of dislocations near the grain boundaries. Therefore, grain boundaries play an important role in

strengthening. Besides, the increased dislocation density during MDIF also led to the substructure strengthening [36]. Both the YS and UTS increased with the grain size decreasing.

Furthermore, the ductility of Ti-6Al-4V alloy was improved due to the achievement of fine-grained structure. Because under the action of the same external force, the strain inside and near the grain boundary of the finer grains varies little and the deformation is more uniform. Thus, the chance of cracking due to stress concentration is much less and larger amount of deformation could be sustained before fracture [39]. Therefore, larger elongation and reduction of section can be obtained. As reported by Wu [40], the toughness and ductility of heavy EH47 plate were significantly improved with grain refinement through inter-pass cooling. In addition, a number of studies reported that the ductility of α+β titanium alloys at room temperature could be improved by the presence of low aspect ratio alpha phase [16,31,41].

As shown in Fig. 10a, when tested at room temperature, the fracture morphology of as-cast Ti-6Al-4V alloy exhibited brittle quasi-cleavage, both quasi cleavage planes and tear ridges were existed, besides, a few dimples were existed. This result was in good agreement with the elongation and percentage reduction of area data. While at high testing temperature of 400 °C, a few more dimples were shown, indicating better plastic deformation behavior at higher temperature. On the contrary, the fracture morphology of Ti-6Al-4V alloy after three steps isothermal forging exhibited typical ductile dimple fracture pattern when tested at both room temperature and 400 °C. When tested at 400 °C, the dimples were bigger and shallower. Above all, these results strongly proved that the MDIF could greatly improve the plasticity of as-cast Ti-6Al-4V alloy.

4. Conclusion

This study investigated the microstructural mechanisms and tensile properties of as-cast Ti-6Al-4V alloy with lamellar starting microstructure during the MDIF. The following conclusions could be draw:

(1) A homogeneous equiaxed grained microstructure with an average grain size of 1.9 μm was achieved after three steps isothermal forging. During MDIF, α lamellae with different orientations of as-cast Ti-6Al-4V alloy were globularized due to the change of loading directions.
(2) The grain refinement mechanism of as-cast Ti-6Al-4V alloy during MDIF included both CDRX and DDRX. The necklaces of new DDRX grains surrounded by HAGBs were formed along the boundaries. Grain subdivision was through CDRX. The fraction of HAGBs increased from 48% to 71%. The recrystallization fraction was increased from 43% to 63% with the isothermal forging steps increasing.
(3) The tensile properties of as-cast Ti-6Al-4V alloy at both room temperature and 400 °C were significantly improved. When tested at both room temperature and 400 °C, the fracture morphology of as-cast Ti-6Al-4V alloy exhibited brittle quasi-cleavage, while the fracture morphology of Ti-6Al-4V alloy after three steps isothermal forging exhibited typical ductile dimple fracture pattern.

Acknowledgments

The authors are grateful for the financial support provided by the National Nature Science Foundation of China (NSFC) (Grant Nos. U1302275 and 51305304) and Fundamental Research Funds for the Central Universities and Major Science and Technology Project “High-end CNC Machine Tools and Basic Manufacturing Equipment” (2013ZX04011061).

References

[1] X. Tan, Y. Kok, Y.J. Tan, M. Descoins, D. Mangelinck, S.B. Tor, K.F. Leong, C.K. Chua, Graded microstructure and mechanical properties of additive manufactured Ti–6Al–4V via electron beam melting, Acta Mater. 97 (2015) 1–16.
[2] S.L. Lu, M. Qian, H.P. Tang, M. Yan, J. Wang, D.H. StJohn, Massive transformation in Ti–6Al–4V additively manufactured by selective electron beam melting, Acta Mater. 104 (2016) 303–311.
[3] Z. Zhao, J. Chen, X. Lu, H. Tan, X. Lin, W. Huang, Formation mechanism of the α variant and its influence on the tensile properties of laser solid formed Ti-6Al-4V titanium alloy, Mater. Sci. Eng. A 691 (2017) 16–24.
[4] Z.X. Zhang, S.J. Qu, A.H. Feng, J. Shen, Achieving grain refinement and enhanced mechanical properties in Ti–6Al–4V alloy produced by multidirectional isothermal forging, Mater. Sci. Eng. A 692 (2017) 127–138.
[5] Z.X. Zhang, S.J. Qu, A.H. Feng, J. Shen, D.L. Chen, Hot deformation behavior of Ti-6Al-4V alloy: effect of initial microstructure, J. Alloys Compd. 718 (2017) 170–181.
[6] Z.X. Zhang, S.J. Qu, A.H. Feng, X. Hu, J. Shen, The low strain rate response of as-cast Ti-6Al-4V alloy with an initial coarse lamellar structure, Metals 8 (2018) 13.
[7] R. Ding, Z.X. Guo, Microstructural evolution of a Ti–6Al–4V alloy during β-phase processing: experimental and simulative investigations, Mater. Sci. Eng. A 365 (2004) 172–179.
[8] J.L.W. Warwick, N.G. Jones, I. Bantounas, M. Preuss, D. Dye, In situ observation of texture and microstructure evolution during rolling and globularization of Ti–6Al–4V, Acta Mater. 61 (2013) 1603–1615.
[9] H. Matsumoto, H. Yoneda, D. Fabregue, E. Maire, A. Chiba, F. Gejima, Mechanical behaviors of Ti–V–(Al, Sn) alloys with α′ martensite microstructure, J. Alloys Compd. 509 (2011) 2684–2692.
[10] L. G, J.C. Williams, Titanium, second ed., Springer, Berlin, 2007.
[11] E.B. Shell, S.L. Semiatin, Effect of initial microstructure on plastic flow and dynamic globularization during hot working of Ti-6Al-4V, Metall. Mater. Trans. A 30 (1999) 3219–3229.
[12] Y. Prasad, T. Seshacharyulu, S.C. Medeiros, W.G. Frazier, Microstructural modeling and process control during hot working of commercial Ti-6Al-4V: response of lamellar and equiaxed starting microstructures, Mater. Manuf. Process. 15 (2000) 581–604.
[13] A.A. Salem, S.L. Semiatin, Anisotropy of the hot plastic deformation of Ti–6Al–4V single-colony samples, Mater. Sci. Eng. A 508 (2009) 114–120.
[14] S.L. Semiatin, T.R. Bieler, The effect of alpha platelet thickness on plastic flow during hot working of Ti-6Al-4V with a transformed microstructure, Acta Mater. 49 (2001) 3565–3573.
[15] T. Seshacharyulu, S.C. Medeiros, W.G. Frazier, Y. Prasad, Microstructural mechanisms during hot working of commercial grade Ti-6Al-4V with lamellar starting structure, Mater. Sci. Eng. A 325 (2002) 112–125.
[16] I. Weiss, F.H. Froes, D. Eylon, G.E. Welsch, Modification of alpha morphology in Ti-6Al-4V by thermomechanical processing, Metall. Trans. A 17A (1986) 1935–1947.
[17] S.L. Semiatin, R.L. Goetz, E.B. Shell, V. Seetharaman, A.K. Ghosh, Cavitation and failure during hot forging of Ti-6Al-4V, Metall. Mater. Trans. A Phys. Metall. Mater. Sci. 30 (1999) 1411–1424.
[18] R.Z. Valiev, R.K. Islamgaliev, I.V. Alexandrov, Bulk nanostructured materials from severe plastic deformation, Prog. Mater. Sci. 45 (2000) 103–189.
[19] R.Z. Valiev, Y. Estrin, Z. Horita, Production bulk ultrafine-grained materials by severe plastic deformation, JOM 58 (2006) 33–39.
[20] H. Margolin, P. Cochen, Titanium '80: Science and Technology, PA, Warrendale, 1980.
[21] S.L. Semiatin, V. Seetharaman, I. Weiss, Flow behavior and globularization kinetics during hot working of Ti-6Al-4V with a colony alpha microstructure, Mater. Sci. Eng. A 263 (1999) 257–271.
[22] T. Seshacharyulu, S.C. Medeiros, J.T. Morgan, J.C. Malas, W.G. Frazier, Y. Prasad, Hot deformation mechanisms in ELI grade Ti-6Al-4V, Scripta Mater. 41 (1999) 283–288.
[23] N. Stefansson, S.L. Semiatin, D. Eylon, The kinetics of static globularization of Ti-6Al-4V, Metall. Mater. Trans. A 33 (2002) 3527–3534.
[24] N. Stefansson, S.L. Semiatin, Mechanisms of globularization of Ti-6Al-4V during static heat treatment, Metall. Mater. Trans. A 34 (2003) 691–698.
[25] S. Zherebtsov, M. Murzinova, G. Salishchev, S.L. Semiatin, Spheroidization of the lamellar microstructure in Ti–6Al–4V alloy during warm deformation and annealing, Acta Mater. 59 (2011) 4138–4150.
[26] G. Lütjering, Influence of processing on microstructure and mechanical properties of (α+β) titanium alloys, Mater. Sci. Eng. A 243 (1998) 32–45.
[27] S.L. Semiatin, V. Seetharaman, I. Weiss, The thermomechanical processing of alpha/beta titanium alloys, JOM 49 (1997) 33–39.
[28] K. Le Biavant, S. Pommier, C. Prioul, Local texture and fatigue crack initiation in a Ti-6Al-4V titanium alloy, Fatig. Fract. Eng. Mater. Struct. 25 (2002) 527–545.
[29] T.B. Britton, F.P.E. Dunne, A.J. Wilkinson, On the mechanistic basis of deformation at the microscale in hexagonal close-packed metals, Proc. Roy. Soc. A Math. Phys. Eng. Sci. 471 (2015) 1–29.
[30] T. Seshacharyulu, S.C. Medeiros, J.T. Morgan, J.C. Malas, W.G. Frazier, Y. Prasad,

Hot deformation and microstructural damage mechanisms in extra-low interstitial (ELI) grade Ti-6Al-4V, Mater. Sci. Eng. A 279 (2000) 289–299.
[31] C.C. Chen, J.E. Coyne, Deformation characteristics of Ti-6Al-4V alloy under isothermal forging conditions, Metall. Trans. A 7 (1976) 1931–1941.
[32] M. Brun, N. Anoshkin, G. Shakhanova, Physical processes and regimes of thermomechanical processing controlling development of regulated structure in the alpha+beta titanium alloys, Mater. Sci. Eng. A 243 (1998) 77–81.
[33] T.R. Bieler, S.L. Semiatin, The origins of heterogeneous deformation during primary hot working of Ti-6Al-4V, Int. J. Plast. 18 (2002) 1165–1189.
[34] L. Meng, P. Yang, F.E. Cui, Z.D. Zhao, Analysis on behavior of dynamic recrystallization in magnesium alloy AZ31 by orientation mapping, J. Univ. Sci. Technol. Beijing 27 (2005) 187–192.
[35] H. Matsumoto, L. Bin, S.-H. Lee, Y. Li, Y. Ono, A. Chiba, Frequent occurrence of discontinuous dynamic recrystallization in Ti-6Al-4V alloy with α' martensite starting microstructure, Metall. Mater. Trans. A 44 (2013) 3245–3260.
[36] T. Sakai, A. Belyakov, R. Kaibyshev, H. Miura, J.J. Jonas, Dynamic and post-dynamic recrystallization under hot, cold and severe plastic deformation conditions, Prog. Mater. Sci. 60 (2014) 130–207.
[37] R.W. Armstrong, The influence of polycrystal grain size on several mechanical properties of materials, Metall. Mater. Trans. 1 (1970) 1169–1176.
[38] I. Sabirov, M.Y. Murashkin, R.Z. Valiev, Nanostructured aluminium alloys produced by severe plastic deformation: new horizons in development, Mater. Sci. Eng. A 560 (2013) 1–24.
[39] J. Toribio, J.C. Matos, B. González, Micro- and macro-approach to the fatigue crack growth in progressively drawn pearlitic steels at different R-ratios, Int. J. Fatig. 31 (2009) 2014–2021.
[40] J.Y. Wu, B. Wang, B.X. Wang, R.D.K. Misra, Z.D. Wang, Toughness and ductility improvement of heavy EH47 plate with grain refinement through inter-pass cooling, Mater. Sci. Eng. A 733 (2018) 117–127.
[41] D. Eylon, C.M. Pierce, Effect of microstructure on notch fatigue properties of Ti-6Al-4V, Metall. Trans. A 7 (1976) 111–121.